JETIR.ORG ISSN: 2349-5162 | ESTD Year : 2014 | Monthly Issue

JOURNAL OF EMERGING TECHNOLOGIES AND INNOVATIVE RESEARCH (JETIR)

An International Scholarly Open Access, Peer-reviewed, Refereed Journal

PARTICLE DISTRIBUTION AS A PROCESS PARAMETER IN POWDER METALLURGY OF HIGH ENTROPY ALLOYS

[1,2] Ch.Chandramouli, [3] B.Venkatesh, [4] M.Manzoor Hussain

[1,2*]Research scholar & Assistant Professor, [3]Professor, [4]Professor

[1,3]Mechanical Engineering Department, Vardhaman College of Engineering, Hyderabad, India
[2]Research scholar, Mechanical Engineering Department, University college of Engineering, JNTUH, Hyderabad, India
[4]Mechanical Engineering Department, University College of Engineering, JNTUH, Hyderabad, India

Abstract : Powder metallurgy has gained prominence for its ability to form alloys with two or more chemically non-reactive elements. Often a majority of components thus formed are made of two primary metals in very fine size compacted under high pressures and sintered at high temperatures. The compaction process is often defined as function of pressure but recent advances in material science have paved way for new kind of metallic compounds made of more than three primary metals, In which case there distribution in given component plays a key role in contributing to its final properties. Current paper aims to propose a methodology to develop such a distribution function as a process parameter using computational model developed by coupling discrete element method and statistical analysis techniques which is further validated using the experimental test rig designed and fabricated as part of the study.

Keywords **Entropy Alloys, computational granulometry, statistical analysis, Powder metallurgy, compaction modeling, R Programming.**

I. INTRODUCTION

Production of components using metal powder has been part of human history since early ages. Egyptians reportedly manufactured tools by compacting powder, Incas were known to produce jewelry using precious metal powder. The iron pillar in Delhi was forged by craftsmen by compacting iron particles into solid unit. The first commercially produced precious metal produced from particles was platinum in late seventeenth century. As Industrial revolution picked up pace, the need for improved mechanical performance became a necessity leading to a renewed interest in powder metallurgy. From copper coins to tungsten carbide tips, this technique has witnessed momentous advancements. The ability to fabricate complex shapes and geometries with minimal finishing requirements has also contributed towards expanding its applications. With recent advances in material science led to a neoteric implementation of this approach utilizing its ability to mix non reacting dissimilar alloying elements using high pressure forging followed by high temperature sintering, thus paving way to a new genre of materials like cemented carbides and high entropy alloys. This process can be divided in three prominent steps:

Powder production: metal powder is produced using mills which blend and bond the particulates to a scale of micro to nano size as per the requisites of final product.

Powder Compaction: a die resembling the final geometry is fabricated and filled with above powder which is uniaxial compressed resulting in a dense compact known as “Green Body” with weak mechanical bonding.

Powder Fusion: the above green body is then sintered using a range of temperatures which is below the melting point of at least one the constituent metals resulting in superlative physical and chemical properties.

Primary drawback observed in above process in non-uniform distribution of tailor made characteristics attributed mainly to irregular compaction of powdered metal which is resultant of difference in hardness, compressibility and thermal expansion of individual elements causing voids and gaps. This is further highlighted in case of high entropy alloys which are made up of more than five metals which in turn forma complex exhibiting attributes of effusive nature such as super and ultra-hardness i.e. materials with Vickers hardness value greater than 40 GPA and 80GPA respectively. All of the above mentioned issues can be restrained using costly experimental characterization or by modeling supported by a fewer number of experiments.

Equation of compaction in powder metallurgy are principal mathematical descriptors correlating various parameters like strength, density, applied pressure, loading conditions, chemical composition, particulate shape, size, relative and absolute porosity, specific surface area and compressibility using correction factors generated based on theoretical and experimental data sets[1,2,3] The need to predict exact pressures of compaction for specific density essential of optimisation of final product can be considered as practical

problem motivating interest of many researchers in developing descriptors to explain the heterogeneous distribution of densification mechanism quantitatively by observing experimental values. (4).A number of empirical equations have been proposed characterizing compressional behavior and densification mechanisms of single phase: metal (Fe, steel, electrolytic Cu, spherical Al, Ni, Mo, Ti, W, atomized Pb and Sn, Ni–Fe alloys etc.) powders, ceramic (graphite, Al2O3, spherical glass, WC, TiC, NbC, SiCetc.) powders or Dual-phase metal-ceramic powders: Al and Cu alloys with(Al2O3, SiC, TiO2 powders), Steel+NbC, , TiH2-SS316L(nano) composite powders[5,6,7,8,9,10].

It is observed that applied compaction pressure contributes predominantly toward modification of elastic properties as they transit from loosely stacked particles to tightly packed solid and this supposedly happens in three stages [11]

In Stage I, the sliding and rearrangement of granules occur,

In Stage II the granules are deformed, and

In Stage III granular densification and hardening happens.

In order to better understand the described behavior, a plethora of microscopic and macroscopic techniques have been published [12]. In the microscopic approach, Grains are often assumed as spheres with different types of contacts [13, 14].Numerous works are focussed on plasticity based compaction models considering a network of axial forces effecting the overall stress and strains variations during cold compaction. [15, 16, 17, 18, 19, 20, 21].These Micro mechanical models highlights the complexity of such physical systems (22). Further there gargantuan need for computational resources makes them an impractical approach to simulate industrial problems.

DEM simulations often produce plenitude of data, the understanding of which is possible through analysis of time dependent variables like particle position, size and wall stresses around them. There are a wide spectrum of commercial [23, 24] and open-source DEM solvers [25, 26, 27] accessible to us even though these packages enable post analysis with certain limitations, executing customized calibrations [28, 29] or post processing modifications is bound by intimate knowledge of internals of programming within existing packages by the user [30]. IDE's like Anaconda circumvent this problem by providing an unified python, SPYDER and R programming interface with a large online community based support consisting fundamental classes and techniques that can be used or altered for performing complex analysis. It uses libraries such as SciPy [31] and NumPy [32, 33] that can accommodate linear algebra and statistical optimization routines, and also provide predefined functions that process DEM output data as NumPy arrays.

II. MATHEMATICAL MODELLING

The modeling of the process is developed using discrete element method where in spherical elements represent metal particles and such an approach is found to be helpful while defining particulate nature and behavior during loading. The interaction of metal powder is in form of contact forces which is modeled using visco-elastic model which is based on Hertz model for elastic contact which takes into account the elastic deformation, viscous dissipation and friction during compaction process. The normal contact force Fn is composed of nonlinear elastic force Fen and viscous component

$$\text{Fdn.} F_n = F_n^e + F_n^d = \frac{4}{3}\bar{E}\sqrt{\bar{r}}\,{u_{rn}^e}^{3/2} + c_n v_{rn} \qquad (1)$$

Where $\bar{E}$is effective young's modulus, $\bar{r}$ is effective radius, u_{rn}^e is particle penetration, c_n is the coefficient of viscosity and v_{rn} normal relative velocity.

$$\frac{1}{\bar{E}} = \frac{1-v_i^2}{E_i} + \frac{1-v_j^2}{E_j} + \cdots \frac{1-v_n^2}{E_n}$$

Where $E_{i\,,j,..n}$ and $v_{i,j,...n}$ are Young's moduli and Poisson's ratio contacting particles respectively and

$$\frac{1}{\bar{r}} = \frac{1}{r_i} + \frac{1}{r_j} + \cdots + \frac{1}{r_n}$$

Where $r_{i,j,...n}$ is contacting particle radii. Further on application of axial load two modes are observed in motion of particles in the die namely deformation and rearrangement by siding and rolling. The strain tensors are defined as

$$\dot{e}_{ij} = \frac{1}{2}\left(\frac{\partial v_i}{\partial x_j} + \frac{\partial v_j}{\partial x_i}\right)$$

Where $v_{i,j}$ are the components of displacement rate associated with the homogenous deformation of a unit cube sitting in a set of Cartesian axes$x_1, x_2\ and\ x_3$. The rate of energy supply by boundary traction is given as$\sigma_{i,j}$, by theorem of virtual work which is either stored as increase in elastic energy $(\dot{U})$ or dissipated as plastic deformation$(\dot{D})$.

$$\sigma_{ij} - \dot{U} - \dot{D} = 0$$

Granular deformation is observed in two modes, elastic and inelastic. Similarly Granular rearrangement occurs through sliding and rolling where in siding is controlled by inter particle friction and rolling is governed by particle deformation mechanism. If $\dot{e}_{ij}^E$ is the components of strain rate due to elastic deformation at contact points, $\dot{e}_{ij}^D$ is strain rate by irreversible deformation at contact patches, $\dot{e}_{ij}^R$ is due to granular rearrangement at contact surface. From energy balance mentioned above $\sigma_{ij}\left(\dot{e}_{ij}^D + \dot{e}_{ij}^R\right) - \dot{D} = 0$ where dissipation energy is given as

$$\dot{D} = \sqrt{\left(k^2\left(\dot{d}_{ij}^D\right)^2 + l^2\,(\dot{e}^D)^2 + \sigma^2\mu^2\left(\dot{d}_{ij}^R\right)^2\right)}$$

Where k, l and μ are adjustable parameters which depend on particle deformation (k, l) and sliding (μ) mechanisms. The energy dissipated at contact patch due to shape change is controlled by 'k', whereas 'l' governs energy dissipated during compaction by deformation. The product of pressure and 'μ' control the frictional energy dissipated due to granular rearrangement. The dilatancy can be defined as $\dot{e}^R = v\sqrt{(\dot{d}_{ij}^R\dot{d}_{ij}^R)}$ Where v is determines dilatancy of bulk granular material. Using above the energy balance can be written as

$$\emptyset \equiv S_{ij}\left(\dot{d}_{ij}^D + \dot{d}_{ij}^R\right) + \sigma\left(\dot{e}^D + v\left(\dot{d}_{ij}^R\dot{d}_{ij}^R\right)^{\frac{1}{2}} - \dot{D} = 0\right.$$

Using envelope theory yield surfaces can be derived using above energy equation. The deviatoric and volumetric components get complicated if dissipation function is not isotropic. This complication can be resolved using lagrangian multiplier. If this multiplier is zero then $\frac{\partial \emptyset}{\partial \dot{e}^D} = \sigma - \frac{l^2 \dot{e}^D}{\dot{D}} = 0$

$$\frac{\partial \emptyset}{\partial \dot{d}_{ij}{}^D} = S_{ij} - \frac{k^2 \dot{d}_{ij}{}^D}{\dot{D}} = 0$$

$$\frac{\partial \emptyset}{\partial \dot{d}_{ij}{}^R} = S_{ij} + \frac{\sigma v \dot{d}_{ij}^R}{\left(d_{ij}^R d_{ij}^R\right)^{\frac{1}{2}}} - \frac{\sigma^2 \mu^2 \dot{d}_{ij}^R}{\dot{D}} = 0$$

Using Flow rule

$$\dot{e}^D = \frac{\sigma \dot{D}}{l^2}$$

$$\dot{d}_{ij}^D = \frac{S_{ij} \dot{D}}{k^2}$$

$$\dot{e}^R = v\left(\dot{d}_{ij}^R \dot{d}_{ij}^R\right)^{\frac{1}{2}}$$

$$\dot{d}_{ij}^R = \frac{S_{ij}}{\frac{\mu^2 \sigma^2}{\dot{D}} - \frac{\sigma v}{\sqrt{\dot{d}_{ij}^R \dot{d}_{ij}^R}}}$$

Using above we get

$$0 = \dot{d}_{ij}^R \dot{d}_{ij}^R \left(\frac{\sigma^2 \mu^2}{\dot{D}}\right)^2 - \frac{2\sigma v \mu^2 \sigma^2 \sqrt{\dot{d}_{ij}^R \dot{d}_{ij}^R}}{\dot{D}} + \left(\sigma^2 v^2 - S_{ij} S_{ij}\right)$$

Which gives

$$\sqrt{\left(\dot{d}_{ij}^R \dot{d}_{ij}^R\right)} = \frac{\sigma v \pm \sqrt{S_{ij} S_{ij}}}{\left(\frac{\sigma^2 \mu^2}{\dot{D}}\right)}$$

As σ is negative, energy dissipated is positive hence using positive root

$$\left(\frac{v\sigma + \sqrt{\left(S_{ij} S_{ij}\right)}}{\sigma^2 \mu^2}\right) \dot{D} = \sqrt{\left(\dot{d}_{ij}^R \dot{d}_{ij}^R\right)}$$

But

$$\frac{S_{ij} S_{ij}}{\frac{\sigma^2 \mu^2}{\dot{D}} - \frac{\sigma v}{\sqrt{\left(\dot{d}_{ij}^R \dot{d}_{ij}^R\right)}}} + \sigma v \sqrt{\left(\dot{d}_{ij}^R \dot{d}_{ij}^R\right)} + \frac{S_{ij} S_{ij} \dot{D}}{k^2} + \frac{\sigma^2 \dot{D}}{l^2} - \dot{D} = 0$$

By eliminating $\dot{d}_{ij}^R$ in above gives the yield function

$$\left(\frac{\left(\left(S_{ij} S_{ij}\right)^{\frac{1}{2}} + v\sigma\right)^2}{(\mu\sigma)^2} + \frac{S_{ij} S_{ij}}{k^2} + \frac{\sigma^2}{l^2}\right)^{\frac{1}{2}} - 1 = \psi_1 = 0$$

If $\left(\left(S_{ij} S_{ij}\right)^{\frac{1}{2}} + v\sigma\right) < 0$ then the above defined yield surface lies outside the yield surface that would have been produced if there was no rearrangement which implies in this region it is easier for particle deformation without any rearrangement and when $\left(\left(S_{ij} S_{ij}\right)^{\frac{1}{2}} + v\sigma\right) > 0$, rearrangement does take place but if $\left(\left(S_{ij} S_{ij}\right)^{\frac{1}{2}} + v\sigma\right) \leq 0$ $\psi_2 = \left(\frac{S_{ij} S_{ij}}{k^2} + \frac{\sigma^2}{l^2}\right)^{\frac{1}{2}} - 1 = 0$, Then above is used and rearrangement does not takes place. Generally the change in k, l and v is caused by amount of granular rearrangement and size of inter granular contact. The initial arrangement is dependent on force applied while filling the die and size of contact depends on mode of powder generation which in turn controlled by granular strengths. Dilatancy depends on disruption of densely packed assemblies of granules and granules rolling away under load due to which after deformation granular material will have new orientation and packing. For better understanding an imaginary intermediate state can be assumed then volume of this notional state is $\dot{V}_{ref} = v_{ref} V_{ref} \left(\dot{d}_{ij}^R \dot{d}_{ij}^R\right)^{\frac{1}{2}}$, where v_{ref} gives the dilation due to breakage of assembly of particulates. To this dilation due to rolling as the contact flattensv_{con} is added. If we assume the v_{ref} is dependent only on difference between the volume V_{ref} and critical volume V_c of sample at which deformation of assemblies occurs without any volume change then$v_{ref} = \eta \frac{(V_c - V_{ref})}{V_c}$, Where η is a constant. If the particle are assumed to be spherical initially and a small amount of flattening takes place then $l = \sigma_g f(\eta)$ where σ_g defines the strength of granules. The current thesis presents a model for both linear and nonlinear hardening, where linear hardening is presented as $l = \sigma\eta$ and nonlinear part is given by $l = A\ (e^{B\eta} - 1)$ where A, B are constants and $k = \alpha l$. The dilatancy due to flattening at contact of round granular is proportional to particle diameter. $v_{con} = m\eta^{\frac{1}{2}}$ Where m is a constant, and total dilatancy is equal to$v_{ref} + v_{con}$

III. COMPUTATIONAL IMPLEMENTATION

Newton's second law can be used to explain the axial compaction of powder while force displacement laws define the movement of particulates during compaction as a function of their position, velocity, and resultant force acting which are updated at end of each time step which is initialised with evaluation of contact between two particles to estimate the number of points overlapping and effecting the magnitude and directionality of force vectors by applying force displacement laws at each point. Then the resultant force and moments are calculated by repeating the same for all particles inside the boundary under consideration. Now using conservation of inertia and momentum, one can estimate the movements in the media. Thus completing one iteration to time cycle and after updating and assuming the new position as initial point the steps are repeated for next iteration until overall movement is near zero or the mentioned time is zero this process is repeated which then can be used to estimate the densification of final state of compressed media. As explicit integration techniques are used the time steps considered are small. The time step value after which the simulation becomes unstable is called critical time step and different criteria's are used for its calculation. In current case we are using Rayleigh critical time step, which is a function of the radius (R), the density (ρ), the shear modulus (G) and the Poisson ratio (υ) of the particles and most commonly used in many publications of powder metallurgy.

$$\Delta T_{Rayleigh} = \frac{\pi R}{0.163v + 0.8766}\sqrt{\frac{\rho}{G}}$$

The displacement of powder particles is calculated by explicitly integration of Newton differential equations of motion

$$m_i \frac{d^2}{dt^2} x_i = \sum_j \left(F_{n,i,j} + F_{t,i,j}\right) + m_i g \;\; \& \;\; I_i \frac{d\omega_i}{dt} = \sum_j T_{ij}$$

Where m_i,I_i, x_i and ω_i are the mass, moment of inertia, position and angular velocity of particle i and $F_{n,i,j}$, $F_{t,i,j}$, T_{ij} are the normal, tangential and torque forces between particles i and j respectively.

$$F_{n,i,j} = F_{n,HM,i,j} + F_{n,cohesion,i,j} \;\; \& \;\; F_{t,i,j} = F_{t,HMi,j}$$

Where $F_{n,HM,i,j}$ and $F_{t,HMi,j}$ are normal and tangential force as per Hertz – Mindlin model.

$$F_{n,HM,i,j} = \frac{4}{3} E_{ij} \delta_{n.i.j}^{\frac{3}{2}} \sqrt{R_{ij}} - \sqrt{\frac{20}{3}} \frac{(\ln e)}{\sqrt{ln^2 e + \pi^2}} \left(m_{ij} E_{ij} \sqrt{R_{ij}\delta_{n,i,j}}\right)^{\frac{1}{2}} v_{n.i.j}$$

$$F_{t,HM,i,j} = \min\left[\mu_{s,i,j} F_{n,HM,i,j}, \left|-8G_{i,j}\delta_{t,i,j}\sqrt{R_{i,j}\delta_{n,i,j}} - \sqrt{\frac{80}{3}} \frac{(\ln e)}{\sqrt{ln^2 e + \pi^2}} \left(m_{i,j} G_{i.j} \sqrt{R_{i,j}\delta_{n.i.j}}\right)^{\frac{1}{2}} v_{t,i,j}\right|\right]$$

Where $\delta_{n,i,j}$, $\delta_{t,i,j}$, $v_{n,i,j}$ and$v_{t,i,j}$ are normal and tangent components overlap and relative velocity components between the particles i and j respectively, $\mu_{s,i,j}$ is the static friction between particle i and j. E_{ij}, G_{ij}, R_{ij} and m_{ij} are equivalent Young's modulus, Shear Modulus, Radius and mass respectively. $\frac{1}{E_{ij}} = \frac{1-v_i^2}{E_i} + \frac{1-v_j^2}{E_j}$, $\frac{1}{G_{ij}} = \frac{2-v_i}{G_i} + \frac{2-v_j}{G_J}$, $\frac{1}{R_{ij}} = \frac{1}{R_i} + \frac{1}{R_j}$, $\frac{1}{m_{ij}} = \frac{1}{m_i} + \frac{1}{m_j}$. The normal cohesion force is given by$F_{n,cohesion,i,j} = K_{ij} A_{ij}$, where $K_{ij}$is the cohesion energy density and A_{ij} is contact are between i and j. The model was implemented using python static and dynamic repositories in Numpy, Scipy, Mathplotlib, PyGRAN and R Programming libraries in Anaconda IDE.

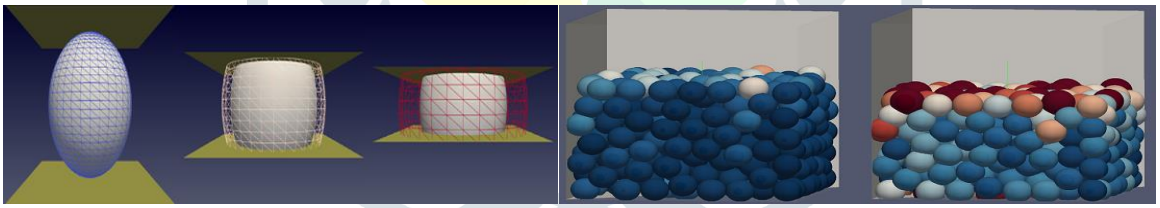

Figure 1 Compaction of Single & Multiple Elements

Developed System stores all conditions defining the state of discrete elements in form of objects properties and methods creating instant classes derived from sub systems as part of main package.

System_obj = System(Element=val , . . . , Elements =[val s])

Classes like particle dimensions and mesh dynamics along with arguments like 'Elements' are user defined, which allows easy handling and representation of diverse dynamics involved in compaction of metal powder. The path to input trajectory is either generated using input string 'Val' or an object of type element. Similarly 'Vals' represent a series of strings or objects.

System_obj = System (P a r t i c l e s =path to pfile, Mesh=path to mfile)

The system creates a new object 'Particle' to store material properties from the input trajectory and 'Mesh' to save node properties from input mesh file. This data is accessible through 'System_obj. Particles' and 'System_obj. Mesh' respectively. For efficiency of system single frame is loaded in to memory at any given time. Functions like 'go to' and 'rewind' helps in further control of frame propagation.

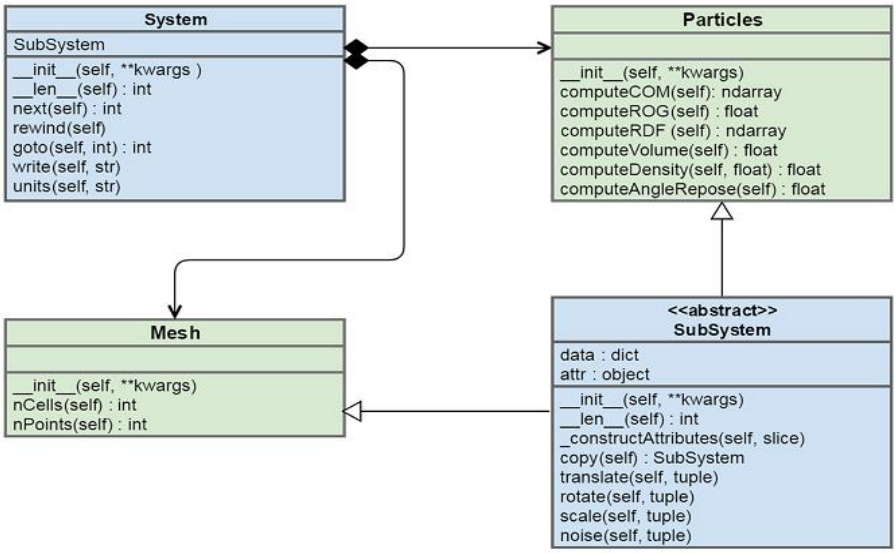

Figure 2 Fundamental class execution in Statistical Analysis Module

In the above the subsystem 'element' stores the attributes in 'System_obj' corresponding to target object. For instance if 'System_obj' contains NumPy array called 'attribute' then 'System_obj[i].attribute' is same as 'System_obj [i]'.
Extending arguments can be attained using concatenation with '+' operator. The array stored in left operand are appended if they occur in right operand. Say if 'Parts_A' and 'Parts_B' are particle objects with NA and NB normal contact surfaces respectively. By performing this operation helps in reducing the attributes by comparing and neglecting commonalities between any given two objects.

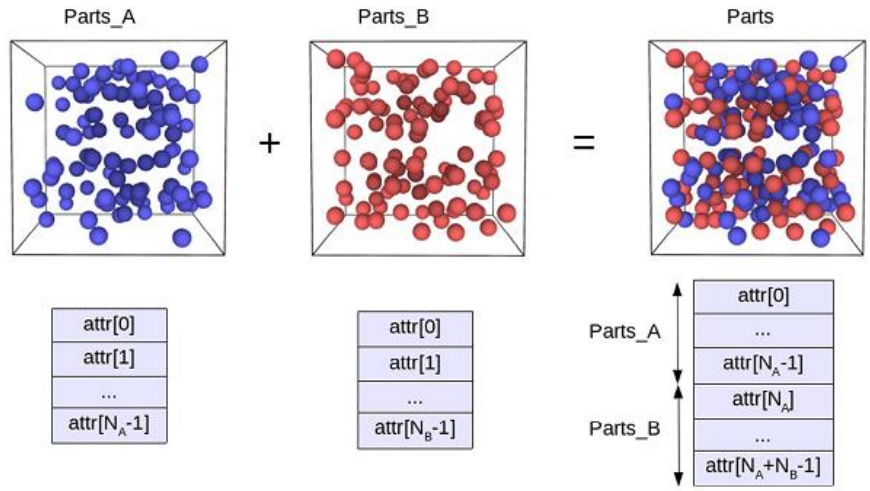

Figure: 3. Addition of two objects with '+' operator

IV. EXPERIMENTAL VALIDATION

The above developed computational model was revalidated using experimental approach where in a die is designed to compact powder of different metals which were milled to a size of 25 Nm using a cylindrical ball mill. The Design Parameters are Working Load: 12 tones, Maximum Load: 20 tones, Load assumed for Die Design: 15 tones based on which designed die dimensions are

1. Base plate: - This is the main body of the die on which loading occurs. The Sample shape is machined as a pocket into the base. Breadth=50mm,Width=48mm,Height=88mm with two holes of diameter 10mm and semicircle of diameter 27.8mm
2. Stud :- Total length=52mm, Head thickness =10mm,Outer diameter of head = 18mm
3. Locking plate: - This is used to hold the sample powder inside the pocket. Breadth=50mm,Width= 24mm, Height= 88mmwith two holes of diameter 10mm
4. Punch: - This is used to apply the desired load on to the sample powder to achieve the required compaction. It has matching negative extrusion of that of the pocket in the base. Height= 44mm, Head diameter=36mm, Semicircle diameter = 27.5mm Die Material: D-2 tool steel with Young's modulus = 210 GPa, Density = 7.7 X 1000 kg/cm^3, Poisson's Ratio = 0.277, Yield Strength = 2200 MPa.

The sample is ball milled high entropy alloy made up of V, Cr, Mn, Nb, Mo, W & C [Graphite] which are processed to nano scale.

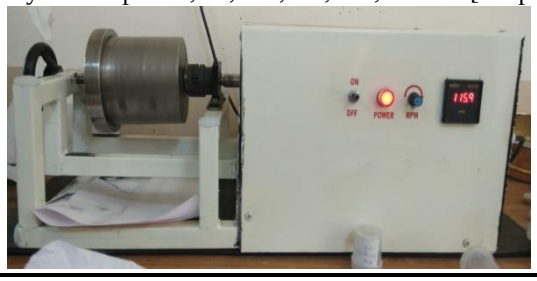

Figure: 4. Ball Mill set up

The steps involved in experimental validation can be described as

- Mixing and blending of powder in ball mill.
- Filling the die with powder mixture.
- Compression of powder mixture in die under hydraulic press.
- Check the mechanical integrity of final sample.

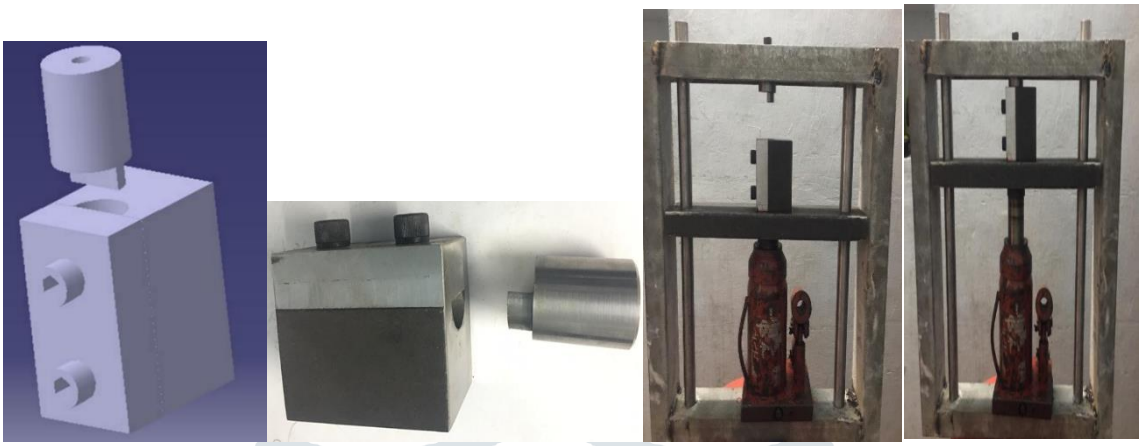

Figure: 5. Final Die Design, Fabricated Assembly & Experimental Setup

V. RESULTS AND DISCUSSION

A Computational model to simulate the compaction of high entropy alloys was developed and validated. Primarily a single element was tested to understand the dynamics and complexities involved in representing such process.

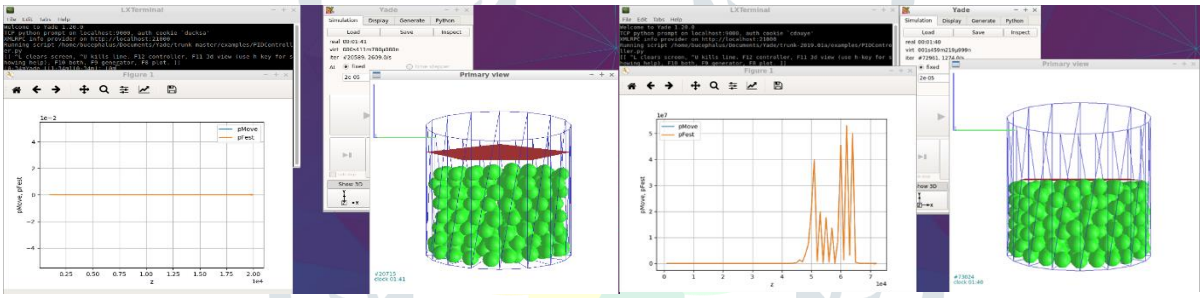

Figure: 6. Singe Element Sample under Compaction

Based on observations from single element test run an arbitrary high entropy alloy made of seven different elements was used to test the developed model. The initial phase involved simulating the settlement of powder in die which then predicted the gravitational, kinetic, elastic, plastic dissipation and inelastic forces acting on the particles during the settling process followed by final stage of settling where other active forces ceased to effect the particulate.

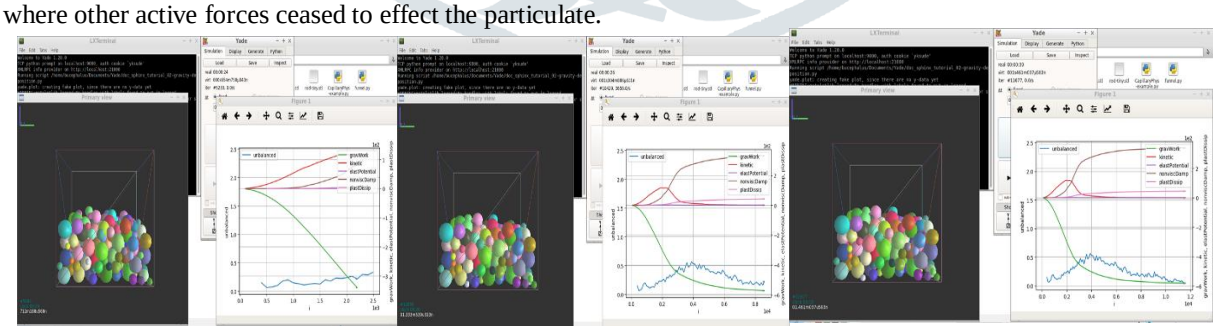

Figure:7. High Entropy Sample Settling in Die

After the settling pattern was observed a machine learning model was developed and used to create a database which in turn would be used to predict the neighboring elements for any given granular particle. This is was then used in final phase of the computation to predict the effective densification of test sample.

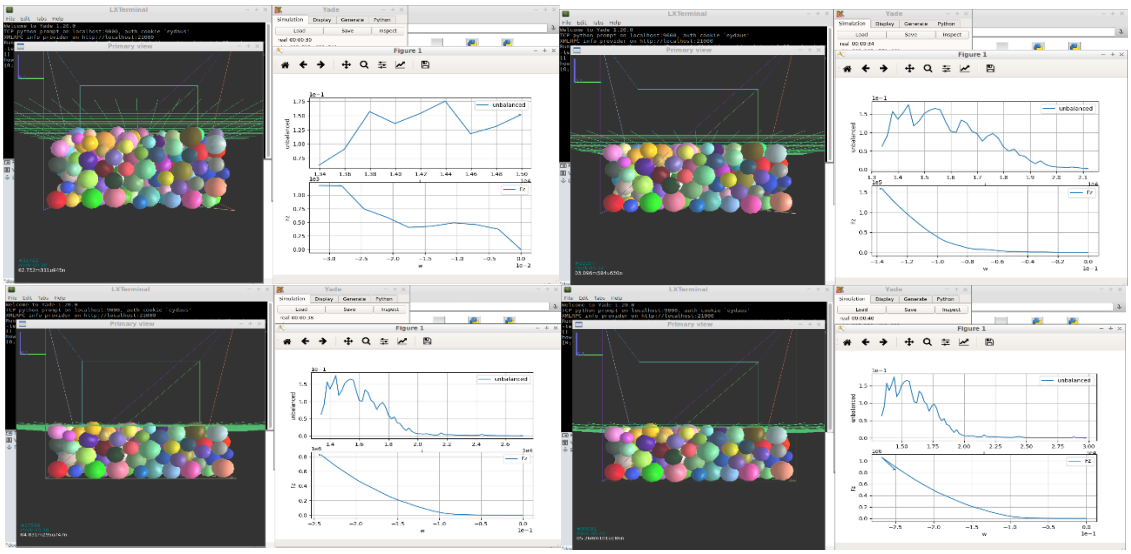

Figure: 8. High Entropy Sample under Compaction

The model predicted the spring back effect due to high hardness values of sample elements.

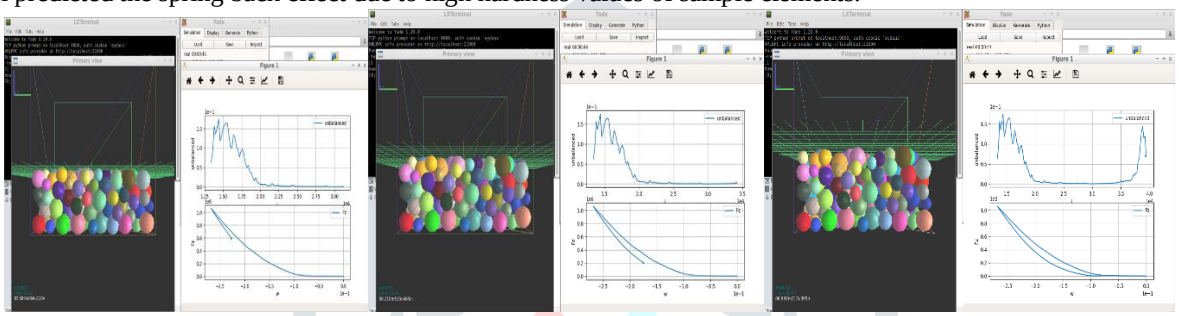

Figure: 9. Spring Back Observed

The model was able to predict the rearrangement due to deformation and rolling along with elastic spring back as the compressive loading was eased. This results were compared with experimental values. When the sample had metals in equal percentages it crumbled due to high hardness the metal underwent less deformability and lacked cohesion as predicted by the computational model. But when the ratios were selected in such a way that the hard metals were less in percentage than relatively softer metals the sample was rigid enough for safe handling and the densification and thickness predicted by the model was near to experimental values.

Figure:10. Crumbled Sample & Final Sample

VI. CONCLUSIONS

The computational model coupled with machine learning model developed using discrete element method and yield function derived by considering deformation and rearrangement of granular particulates for high entropy alloys is found to be accurately validated by experimental values and the approach of using machine learning technique's to predict the arrangement pattern of elements is helpful in bringing down the computational resource required. Further this method is helpful in understanding the dynamics of such complex systems. Feasibility of similar approach for simulating sintering process needs to be studied and a complete model to predict the final properties of high entropy alloys computationally.

VII. ACKNOWLEDGMENT

Thepreferredspellingoftheword "acknowledgment" inAmericaiswithoutan "e" afterthe "g".Avoidthestiltedexpression, "Oneofus(R.B.G.)thanks..."
Instead,try"R.B.G.thanks".Putapplicablesponsoracknowledgmentshere;DONOTplacethemonthefirstpageofyourpaperorasafootnote.

REFERENCES

[1] A normalized density-pressure Curve for Powder Compaction. Heckel, R. W. 1962, Trans. Metall. Soc. AIME, 224.

[2] Relationship between compacting pressure, green density, and green strength of copper powder compacts. I. H. Moon, K. H. Kim. 1984, Powder Met., 27(2), pp. 80-

[3] A New Powder Compaction Equation. Rong-de, Ge. 1991, the International Journal of Powder Metallurgy, 27, pp. 211-214.
[4] An Overview of Compaction Equations. Çomoğlu, T. 2007, J. Fac. Pharm, Ankara,, pp. 123-133.
[5] Quantification of Metal Powder Compressibility in Uniaxial Compaction. L. Parilák, E. Dudrová, R. Bidulský, M. Kabátová. Vienna: s.n., 2004. Metallurgy World Congress and Exhibition. pp. 593-598.
[6] Compressibility Evaluation Of Mechanically Activated Niobium And Aluminum Powders Mixtures. M. Castagnet, R. B. Falcão, R. M. Leal Neto. Brasil: s.n., 2008. CBECiMat.
[7] Analysis of the compaction behavior of Al–SiC nanocomposites using linear and non-linear compaction equations. H. Hafizpour, A. Simchi, S. Parvizi. 2010, Advanced Powder Technology.
[8] Compressibility of Fe/SiO2 Coated Composite Powders. A. Miskova, E. Dudrova, H. Brunckova, M. Faberova, R.Bures. 2010. World Congress - Fundamentals of Pressing. p. 39.
[9] Evaluation of compaction equations and prediction using adaptive neuro-fuzzy inference system on compressibility behavior of AA 6061 100− x–x wt.% TiO 2 nanocomposites prepared by mechanical alloying. S. Sivasankaran, K. Sivaprasad, R. Narayanasamy, V. K.Iyer. 2011, Powder Technol.
[10] Analysis of the Cold Compaction Behaviour of TiH2-316L Nanocomposite Powder Blend Using Compaction Models. C. Machio, R. Machaka, T. Shabalala, H. K. Chikwanda. 2015, Materials Science Forum,, pp. 828-829.
[11] An elastoplastic framework for granular materials becoming cohesive through mechanical densification. Part I–small strain formulation. . Piccolroaz, A. , Bigoni, D. , Gajo, A. ,. 2006, European Journal of Mechanics-A/Solids 25 (2), pp. 334-357.
[12] Die compaction of copper powder designed for material parameter identification. Bier, W., Dariel, M. , Frage, N. , Hartmann, S. , Michailov, O. ,. 2007. , Int. J. Mech. Sci. 49 (6), , pp. 766–777 .
[13] The influence of an increasing particle coordination on the densifica- tion of spherical powders. Arzt, E. 1982, Acta Metall. 30 (10), pp. 1883–1890.
[14] Constitutive modelling of powder compaction–i. theoretical concepts. Cocks, A. , Sinka, I. ,. 2007, Mech. Mater. 39 (4), pp. 392–403.
[15] Yielding of metal powder bonded by isolated contacts. Fleck, N.A. , Kuhn, L.T. , McMeeking, R. 1992, J. Mech. Phys. Solids 40 (5), pp. 1139–1162.
[16] On the cold compaction of powders. Fleck, N. 1995, J. Mech. Phys. Solids. 43 (9, pp. 1409–1431.
[17] Compaction of an array of spherical particles. Ogbonna, N. , Fleck, N. 1995, Acta Metall. Mater. 43 (2, pp. 603–620.
[18] The viscoplastic compaction of powder. Fleck N, Storåkers, B. , McMeeking, R. s.l. : Springer, 1997. IUTAM Symposium on Mechanics of Granular and Porous Materials. pp. 1–10.
[19] Yield behaviour of cold compacted composite powders. Sridhar, I. , Fleck, N. 2000, Acta Mater. 48 (13, pp. 3341–3352.
[20] Constitutive modelling of powder compaction and sintering. Cocks, A.C. 2001, Prog. Mater. Sci. 46, pp. 201–229.
[21] Constitutive modelling of powder compaction–i. theoretical concepts. Cocks A, Sinka, I. 2007, and Mech. Mater. 39 (4, pp. 392–403.
[22] Cold plastic compaction of powders by a network model. Heyliger P, Mc Meeking, R. 2001, J. Mech. Phys. Solids 49 (9, pp. 2031–2054.
[23] Solutions, DEM. EDEM User Guide. 2018.
[24] CD-Adapco. STAR-CCM+ User Guide. 2018.
[25] YADE-OPEN DEM: an open-source software using a discrete element method to simulate granular material. Kozicki J, Donzé F. 2009, Eng Comput 26(7):, pp. 786-805.
[26] Scaling benchmark of ESyS particle for elastic wave propagation simulations. Weatherley DK, Boros VE, Hancock WR, Abe S. s.l. : IEEE, 2010. IEEE sixth international conference on. pp. 277–83.
[27] LIGGGHTS-open source discrete element simulations of granular materials based on Lammps. Kloss C, Goniva C. 2011. Supplemental proceedings: Materials fabrication, properties, characterization, and modeling, Volume 2.
[28] A methodical calibration procedure for discrete element models. Rackl M, Hanley KJ. 2017, Powder Technol 307, pp. 73-83.
[29] Probabilistic calibration of discrete element simulations using the sequential quasi-monte Carlo filter. Cheng H, Shuku T, Thoeni K, Yamamoto H. 2018, Granul Matter 20(1):11.
[30] Visualization and analysis of atomistic simulation data with OVITO-the open visualization tool. . A., Stukowski. 2009, Modelling Simulation Mater Sci Eng 18(1):015012.
[31] Jones E, Oliphant T, and Peterson P. SciPy: Open source scientific tools for Python. Scipy. [Online] 2001. http://www.scipy.org.
[32] TE. Oliphant. A guide to NumPy, Vol. 1. USA: Trelgol Publishing, 2006.
[33] The NumPy array: a structure for efficient numerical computation. . Walt Svd, Colbert SC, Varoquaux G. 2011, Comput Sci Eng 13(2), pp. 22-30.

[1] Ali, A. 2001.Macroeconomic variables as common pervasive risk factors and the empirical content of the Arbitrage Pricing Theory. Journal of Empirical finance, 5(3): 221–240.
[2] Basu, S. 1997. The Investment Performance of Common Stocks in Relation to their Price to Earnings Ratio: A Test of the Efficient Markets Hypothesis. Journal of Finance, 33(3): 663-682.
[3] Bhatti, U. and Hanif. M. 2010. Validity of Capital Assets Pricing Model.Evidence from KSE-Pakistan.European Journal of Economics, Finance and Administrative Science, 3 (20).